Extremophiles (2011) 15:359–364
DOI 10.1007/s00792-011-0367-2

ORIGINAL PAPER

Conserved residues in membrane-bound acid pyrophosphatase from *Sulfolobus tokodaii*, a thermoacidophilic archaeon

Fumitoshi Manabe · Hirofumi Shoun · Takayoshi Wakagi

Received: 18 November 2010 / Accepted: 8 March 2011 / Published online: 2 April 2011

Abstract A membrane-intrinsic acid pyrophosphatase (ST2226) from *Sulfolobus tokodaii*, a thermoacidophilic archaeon, is possibly involved in glycoprotein biosynthesis and belongs to the phosphatidic acid phosphatase class 2 superfamily, including both membrane-intrinsic and soluble enzymes with divergent functions ranging from dephosphorylation of undecaprenylpyrophosphate and phospho-monoesters such as glucose-6-phosphate to vanadium-containing chloroperoxidation. ST2226 is an archaeal ortholog of these enzymes sharing a common phosphatase motif. Through site-directed mutagenesis as to each of the conserved residues, the catalytic roles of the latter were deduced, as well as the transmembrane topology with all the conserved residues in close proximity to the outside of the membrane.

Keywords Phosphatase motif · Pyrophosphatase · Dolicholpyrophosphatase · Membrane integral enzyme · Archaea

Introduction

In recent years, a common phosphatase motif, K(X_6)RP($X_{12–54}$)PSGH($X_{31–54}$)SR(X_5)H(X_3)D, has been reported in several groups of enzymes such as bacterial nonspecific acid phosphatases including PhoN from *Salmonella typhymurium* and its ortholog Pho from *Escherichia blattae*, several membrane-bound "acid pyrophosphatases" belonging to the PAP2 (phosphatidic acid phosphatase type 2) superfamily that possibly play a role as undecaprenylpyrophosphate phosphatases in bacterial peptide glycan synthesis, mammalian glucose-6-phosphatase (G6Pase) bound to the endoplasmic reticulum membrane that plays a key role in glucose homeostasis, and vanadium-containing chloroperoxidase (VCPO) from the plant pathogenetic fungus *Curvularia inaequalis* (Stukey and Carman 1997; Hemrika et al. 1997). The structural relationship between "lipid phosphatases" and VCPO (Neuwald 1997), and structural and functional comparisons between bacterial acid phosphatases, VCPO and vanadium bromoperoxidase (VBPO) found in red and brown algae, have been reported (Littlechild et al. 2002).

Three-dimensional structures have been reported for *C. inaequalis* VCPO (PDB ID: 1IDQ) (Messerschmidt and Wever 1996), *Corallina officinalis* VBPO (Isupov et al. 2000), *E. blattae* Pho (PDB ID: 1EOI) (Ishikawa et al. 2000), *S. typhymurium* PhoN (PDB ID: 2A96) (Makde et al. 2007), and so on. These enzymes are soluble proteins.

Based on these reports, a common structural and functional feature of the phosphatase family appears to be established for soluble enzymes, but the three-dimensional structure of membrane-bound enzymes remains unknown.

The membrane-bound undecaprenylpyrophosphate phosphatases required for bacterial peptide glycan synthesis, such as PgpB (Icho 1988; El Ghachi et al. 2005; Touze et al. 2008) and YbjG (Tatar et al. 2007) from *Escherichia coli*, and BcrC (Bernard et al. 2005) and SubG (Wu et al. 2006) from *Bacillus subtilis* (referred to as "acid pyrophosphatase", "lipid phosphatases", or PAP2 enzymes), have been extensively studied. These enzymes are integral-membrane proteins and unable to hydrolyze phosphate mono-esters such as *p*-nitrophenylphosphate (pNPP) (Touze et al. 2008).

Communicated by A. Driessen.

F. Manabe · H. Shoun · T. Wakagi (✉)
Department of Biotechnology, The University of Tokyo, 1-1-1 Yayoi, Bunkyo-ku, Tokyo 113-8657, Japan
e-mail: atwakag@mail.ecc.u-tokyo.ac.jp

Membranes from *S. tokodaii*, a thermoacidophilic archaeon growing optimally at pH 2–3 and 75–80°C, show unique enzyme activity that hydrolyzes PPi, ATP, and ADP, at an optimal pH of 2–3 (Fig. 2) (Wakagi and Oshima 1985, 1986). Solubilization and purification of the enzyme from membranes of *S. tokodaii* (Amano et al. 1993) and *Sulfolobus acidocaldarius* (Meyer and Schäfer 1992), and identification of the gene (Moll and Schäfer 2004) and gene expression system in *Escherichia coli* have been reported (Manabe et al. 2009). The enzyme from *S. tokodaii*, ST2226, the archaeal homolog of the PAP2 superfamily, possibly corresponds to a dolicholpyrophosphate phosphatase that is included in the glycosylation system of membrane proteins (Eichler and Adams 2005). ST2226 hydrolyzes PPi, ATP, ADP, and geranylpyrophosphate (C_{10}PP). C_{10}PP is dephosphorylated to geranylphosphate, which is not hydrolyzed by ST2226, suggesting that ST2226 is not a nonspecific phosphatase and possibly catalyzes the dephosphorylation of dolicholpyrophosphate during the protein glycosylating "dolichol cycle" (Manabe et al. 2009).

In the previous paper we constructed four mutants which deleted Arg2, Arg2-Lys3, 66 residues (position 4–69) and 72 residues (position 4–75), to see if the positive charge in the inside loop are required for integration of membrane. The present work aimed to investigate the role of conserved residues in the "common phosphatase motif" in ST2226 by site-directed mutagenesis since an archaeal counterpart of a PAP2 family enzyme has not been studied in detail to date. The residues include Pro103, Pro122, Ser123, His125, Ser158, Arg159, Gly163, His165, Pro167, and Asp169. Lys95 or Pro102 were not included since they are not conserved in certain member(s) of PAP2 family as shown in Fig. 1. Alignment of the amino acid sequence and topology of ST2226 were re-evaluated.

Materials and methods

Expression plasmids for the wild type and variant enzymes

The plasmid used to express wild type ST2226 was pSTH, and the host was *E. coli* BL21(DE3) CodonPlus-RIL, as described previously (Manabe et al. 2009). The oligonucleotides used to construct variant enzymes are shown in Table 1. Mutations were introduced by the QuikChange method (Stratagene) using pSTH as a template. The nucleotide sequences of the plasmids were confirmed with a CEQ2000XL DNA analysis system (Beckman Coulter). The recombinant enzymes were each expressed as a C-terminal fusion of 24 amino acid residues with HSV-tag and His_6-tagged extensions at the *Xho*I site of the pET25b(+) vector (Novagene).

Preparation of recombinant *E. coli* membranes

Recombinant *E. coli* was cultured in Luria–Bertani medium with appropriate antibiotics. The cells were collected and then sonicated to obtain a membrane fraction through two steps of centrifugation as previously described (Manabe et al. 2009).

Assaying of activity and protein amount

Acid pyrophosphatase activity was determined at 70°C in 50 mM phthalate buffer, pH 3.0, 1 mM PPi and an

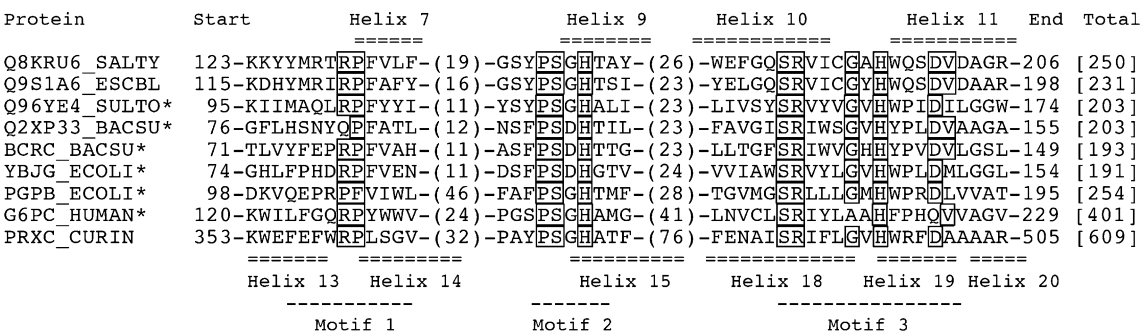

Fig. 1 Alignment of sequences of ST2226 and related proteins. The names of proteins are shown by UniProtKB database entry name. Q8KRU6_SALTY, *Salmonella typhimurium* acid phosphatase PhoN (PDB ID: 2A96); Q9S1A6_ESCBL, *Escherichia blattae* acid phosphatase (PDB ID: 1EOI); Q96YE4_SULTO, *Sulfolobus tokodaii* membrane-bound acid pyrophosphatase, ST2226; Q2XP33_BACSU, BsSubG, *Bacillus subtilis* acid phosphatase homolog SubG; BCRC_BACSU, *B. subtilis* undecaprenylpyrophosphatase BcrC; YBJG_ECOLI, *Escherichia coli* undecaprenylpyrophosphatase YbjG; PGPB_ECOLI, *E. coli* undecaprenylpyrophosphatase PgpB; G6PC_HUMAN, human glucose-6-phosphatase; PRXC_CURIN, *Curvularia inaequalis* chloroperoxidase (PDB ID: 1IDQ). Conserved residues are *boxed*. Numbers in *parentheses* show gap lengths, and those in *square brackets* total residues. Known integral membrane proteins are denoted by *asterisks*. Helices 7–11 in *S. typhyimurium* PhoN are indicated above the sequence, and helices 13–20 in *C. inaequalis* chloroperoxidase are indicated below the sequence. Motifs 1, 2, and 3 correspond to Domains 1, 2, and 3 (Stukey and Carman 1997), or Motifs A, B, and C (Neuwald 1997), or Motifs C1, C2, and C3 (Touze et al. 2008), respectively

Table 1 Oligonucleotide primers used to construct variant enzymes

Primer	Nucleotide sequence
P103A	5′-GGCTCAATTAAGGgCTTTCTATTATATACATGCTGACC-3′
P122A	5′-CCACATGATTATAGTTATgCTTCTGGTCACGCTTTAATTG-3′
S123A	5′-GATTATAGTTATCCTgC*TGGcCA*CGCTTTAATTGTAGG-3′
H125A	5′-GATTATAGTTATCCTTCT*GGcgcC*GCTTTAATTGTAGGTGATGG-3′
S158A	5′-GCTTTGATAGTAT*CaTATg*CTAGAGTTTATGTTGGTG-3′
R159A	5′-GATAGTATCTTATT*CTgcAG*TTTATGTTGGTGTTCATTG-3′
G163A	5′-CTAGAGTTTATGTTGcTGTTCATAGGCCTATTGATATTC-3′
H165A	5′-CTAGAGTTTATGTTGGTGTTgcTTGGCCTATTGATATTCTAGG-3′
P167A	5′-GTTGGTGTTCATTGGgCT*AtcGAT*ATTCTAGGTGGTTGG-3′
D169A	5′-GTTGGTGTTCAT*TGGCCa*ATTGcTATTCTAGGTGGTTGGC-3′

Underlines show the nucleotide sequences to induce amino acid replacements. Small letters show replaced nucleotides. Italics show the restriction site used to confirm the mutated plasmids. Oligonucleotides with complementary sequences were also used for mutagenesis

appropriate amount of membrane fraction. The reaction was started by addition of membranes and stopped by cooling on ice. Released Pi was determined by adding BIOMOL GREEN Reagent (BIOMOL Research), and absorbance at 620 nm was measured as described previously (Manabe et al. 2009). One unit of activity was defined as 1 μmol release of Pi per min in initial velocity of the reaction. The protein concentration was determined by the BCA (bicinconinic acid) method (Pierce) as described previously (Manabe et al. 2009).

Recombinant *E. coli* membranes (50 μg protein) were subjected to SDS-14% acrylamide gel electrophoresis and then trans-blotted onto polyvinylidene fluoride (PVDF) membranes (Millipore). The membranes were first incubated with mouse anti-His_6-tag antibodies and then with alkaline phosphatase conjugated anti-mouse IgG antibodies (Western Breeze, Invitrogen). The immunocomplex was visualized by enzyme reaction using substrates, BCIP/NBT, included in the reagent kit.

The relative units of acid PPase activity was normalized as to PPase protein expression, as determined from the staining intensity of the PPase band (in arbitrary units) on Western blotting with anti-His_6-tag antibodies. The peak area of PPase was calculated using imageJ software. The relative specific activity of a variant PPase was calculated by dividing the total activity by the relative amount of the PPase contained in the membrane preparation.

Results and discussion

Alignment and topology

Amino acid sequence alignment of ST2226 and related enzymes is shown in Fig. 1. Based on the three-dimensional structures of *S. typhymurium* PhoN (231 residues, PDB ID: 2A96), *E. blattae* Pho (230 residues, PDB ID: 1EOI), and *C. inaequalis* VCPO (609 residues, PDB ID: 1IDQ), the secondary structures of these enzymes are also indicated by double bars in Fig. 1. The conserved residues boxed in Fig. 1 are divided into three groups, motifs 1, 2, and 3. These residues are located in close proximity to form the active site of the enzyme. Based on this, conserved residues for membrane-bound enzymes are assumed to be located on the same side of the membrane. In ST2226, the enzyme shows an optimal pH of 2–3, which is equal to the extracellular pH, suggesting clearly that the conserved residues should be located on the outside of the membrane, if they are catalytically important.

The deduced topology of ST2226 is shown in Fig. 2a. The previous model with 5 trans-membrane helices was based on a hydropathy plot and modified according to the tendency to basic residues inside and acidic residues outside, which could be favorable for a large pH difference across the membrane. In contrast, the new topology model, with six membrane-spanning segments (residues 4–24, 34–54, 76–96, 122–139, 143–162, and 167–186), with three outside loops (residues 25–33, 97–121, and 163–166), containing all the conserved residues in close proximity so that they can catalyze the hydrolysis of a substrate on the outside of the membrane, is based on structure modeling of the active site region (Fig. 2b) created by the crystal structure of the corresponding region of *S. typhimurium* PhoN complexed with phosphate (Fig. 2c).

Membrane spanning topologies of PAP2 family enzymes have been deduced for G6Pase (9 trans-membrane helices) (Ghosh et al. 2002) and proposed based on the experimental background for YbjG (5 transmembrane helices) (Tatar et al. 2007) and PgpB (6 trans-membrane helices) (Touze et al. 2008) from *E. coli*. In these topology models, the three phosphatase motifs are located on the outside of the membrane. In contrast, in our topology model (Fig. 2a), certain conserved residues (such as Pro122, Sr123, His125 Ser158, and Arg159) are not completely exposed to the outside. This may be applicable because the hydrophobic substrate such as dolicholpyrophosphate is buried in the membrane. The helices in ST2226 which correspond to helices 6, 9, 10, and 11 in

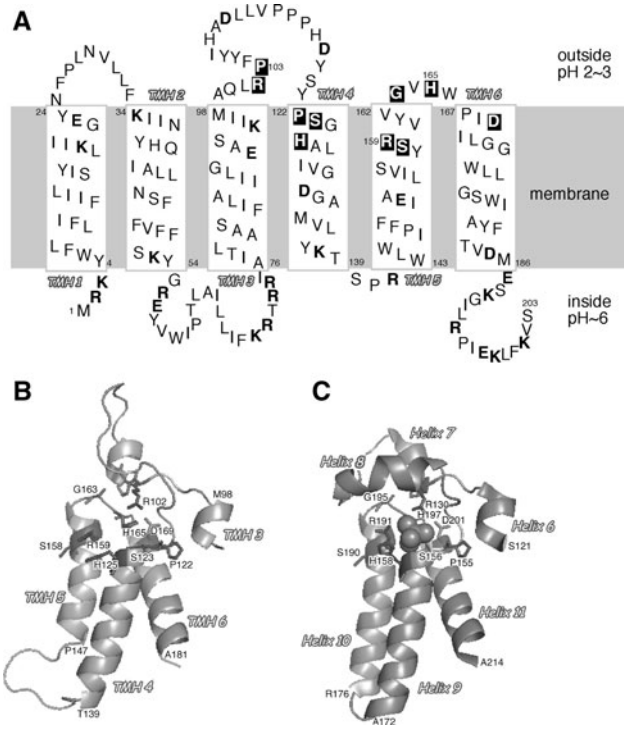

Fig. 2 Deduced structure of ST2226. **a** Proposed topological model of ST2226. Basic and acidic residues are in *bold letters*. Conserved residues are *highlighted*. **b** Structure model of the active site region (position 95–181) of *S. tokodaii* acid pyrophosphatase ST2226 constructed by using **c** crystal structure of *S. typhimurium* PhoN (PDB ID: 2A96, position 121–214) with bound phosphate (indicated by *spheres*) as a template

Salmonella PhoN (Figs. 1, 2c) are designated as transmembrane helices (TMHs) 3, 4, 5, and 6, respectively (Fig. 2a, b). Since PhoN is a soluble protein, exact arrangement of ST2226 TMHs may not be the same as shown in Fig. 2b. Nevertheless, the conserved residues are clustered together in close proximity, and binding of phosphate, a possible moiety of substrate, is allowed in this model.

Expression of variant PPases

The residues replaced with Ala were Pro103, Pro122, Ser123, His125, Ser158, Arg159, Gly163, His 165, Pro167, and Asp169. Fifty micrograms of protein of recombinant *E. coli* membranes was subjected to SDS-PAGE and then Western-blotted on to a PVDF membrane, followed by visualization of the His-tagged protein. The results are shown in Fig. 3. One major band appeared in each lane at around 25 kDa, which corresponds to recombinant PPase. A smaller band at around 12 kDa also appeared for the D169A mutant, which may be a proteolytic fragment of PPase trapped in the membrane preparation. The expression level of PPase varied from 49 to 165% of that of the

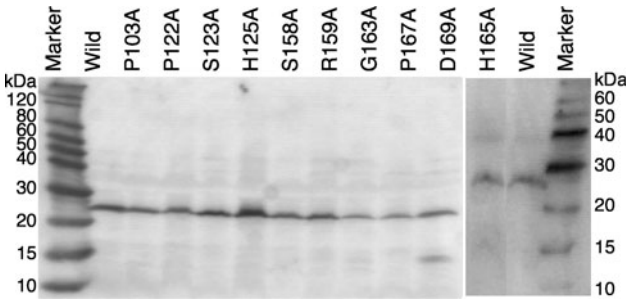

Fig. 3 SDS-PAGE of recombinant *E. coli* membranes. Expression of variant PPases estimated by Western blotting, as detected with anti-His_6 antibodies

wild type enzyme (Table 2). The amount of PPase protein expressed can be deduced from the staining intensity of each lane in Fig. 3. The peak area corresponding to 25 kDa was measured by scanning with ImageJ software (http://rsb.info.nih.gov/ij). The ratio of the peak area of the variant to that of the wild type was calculated. The total PPase amount was expressed in arbitrary units assuming that the amount of the wild-type PPase is 1.

PPase activity of variant enzymes

The specific activity of each variant PPase was thus estimated, as summarized in Table 2.

The variants showed specific activity of 0.02–0.71 U/mg total membrane protein, while membranes from *E. coli* where the wild type recombinant enzyme is being expressed showed that of 4.52 U/mg.

H165A showed the lowest and practically null activity (0.4% of wild type level). This residue corresponds to His189 in the catalytic site of *E. blattae* acid phosphatase and to His496 in the center of the catalytic site to which the vanadium atom of VCPO was bound.

His165 in ST2226 corresponds to His176 in human G6Pase (Fig. 1). Human G6Pase, upon incubation with [^{32}P]G6P, was labeled with ^{32}P. The phosphorylated intermediate was stable enough to isolate a labeled fragment, and the labeled residue was determined to be His176. His119 and Arg170 assist incorporation of ^{32}P to His176, which is a catalytic nucleophile. Variants K76N, R83C, H119A, R170Q, and H176A had completely lost the activity (Ghosh et al. 2002).

Such a phosphorylated intermediate is assumed also for apo-VCPO, in which His496 is phosphorylated. A cofactor vanadate, HVO_4^{2-}, covalently binds to His496 in the catalytic site of VCPO, which is facilitated by Lys353, Arg360, and Arg490. Phosphatase activity was observed for apo-VCPO, in which the phosphate moiety of the substrate replaces vanadate (Renirie et al. 200a, b). Not only is His496 important but variant VCPOs with K353A

Table 2 Activity of variant PPases

	Specific activity (U/mg)[a] (1)	Net specific activity(U/mg)[a] (1)–0.07 (2)	Relative amount of PPase[b] (3)	Relative specific activity of PPase (%) [(2)/(3)]/4.52 × 100
Wild (pSTH)	4.59 ± 0.418	4.52	1	100
P103A	0.22 ± 0.021	0.15	0.91	3.3
P122A	0.43 ± 0.046	0.36	0.98	8.0
S123A	0.78 ± 0.061	0.71	1.32	16
H125A	0.41 ± 0.040	0.34	1.65	7.5
S158A	0.16 ± 0.022	0.09	0.79	2.0
R159A	0.12 ± 0.020	0.05	1.00	1.1
G163A	0.21 ± 0.047	0.14	0.49	3.1
H165A	0.09 ± 0.027	0.02	0.68	0.4
P167A	0.15 ± 0.016	0.08	0.50	1.8
D169A	0.15 ± 0.011	0.08	0.78	1.8
Control[c]	0.07 ± 0.014	0	–	–

[a] Specific activity in units per mg of total membrane protein

[b] Variant PPase amount in arbitrary units, compared to wild type PPase, as calculated from the intensity of the band in Fig. 3

[c] Control value obtained with membranes from *E. coli* bearing pET25b(+)

and R360A show decreased phosphatase activity, i.e., only about 10% of the wild type level (Renirie et al. 200a, b).

Thus, His176 in G6Pase, His496 in VCPO, and His167 in *Salmonella* PhoN correspond to His165 of ST2226, all of which being essential for enzyme activity, possibly as a catalytic nucleophile.

Based on these findings, the function of conserved residues in ST2226 can be deduced as follows: Arg102 and Arg159 bind the substrate phosphate group through ionic interactions. In fact, R159A showed a significant decrease (to 1% of the wild type level) in PPase activity.

R159A and D169A also showed decreased activity, suggesting that Arg159 and Asp169 stabilize the transition state of the phosphatase reaction. Replacement of His125, a possible proton donor, with Ala left 10% remaining activity (Table 2). Other mutants of ST2226 showed PPase-specific activities of between 3.3 and 16% of that of wild type membranes.

Pro103 and Pro122 are adjacent to Arg102 and Ser123, respectively, which possibly bind phosphate (Fig. 2b). Loss of PPase activity in P103A and P122A may result from disturbance of the active site scaffold which should be maintained by these conserved Pro residues. The role of Arg191 in *Salmonella* PhoN is to restrict the active site conformation of His158 and His197 (Makde et al. 2007). Side chain of Ser190 adjacent to this Arg191 swung out of the active site of PhoN (Fig. 2c). In ST2226, the side chain of the corresponding Ser158 also turns outward (Fig. 2b), and S158A shows 2% of the wild-type membrane activity (Table 2). Since this Ser is conserved among the PAP2 family enzymes, it may interact with other residues in a different trans-membrane helix, stabilizing the topology of the enzyme.

Conclusion

Membrane-intrinsic ST2226, an archaeal ortholog of the PAP2 family enzymes, catalyzes Mg-independent hydrolysis of PPi and C_{10}PP at extracellular pH, but does not hydrolyze AMP, G6P, or pNPP, indicating that it is not a nonspecific phosphatase. In these respects, it is similar to *E. coli* membrane-intrinsic acid pyrophosphatases such as YbjG and PgpB, which recycle periplasmic undecaprenylpyrophosphate during peptideglycan synthesis. This study revealed that ST2226, possibly playing a role in dolicholpyrophosphate hydrolysis in glycoprotein biosynthesis, has catalytic site residues quite similar to those of other members of the phosphatase family in function and topological localization.

However, it is different from membrane-intrinsic G6Pase, soluble and nonspecific acid phosphatase and VCPO in substrate specificity, although they share a common phosphatase motif composed of three motifs. Therefore, the question remains of why pNPP can be hydrolyzed by PhoN and CPO, but not by ST2226 or *E. coli* PgpG. The former two are soluble enzymes with wide specificities for phosphomonoesters, while the latter two are membrane integral enzymes possibly related to the biosynthesis of peptideglycans or glycoproteins. This

question may be directly related to the physiological roles of these enzymes. Further analysis of their function and structure is necessary.

References

Amano T, Wakagi T, Oshima T (1993) An ecto-enzyme from *Sulfolobus acidocaldarius* strain 7 which catalyzes hydrolysis of inorganic pyrophosphate, ATP, and ADP: purification and characterization. J Biochem 114:329–333

Bernard R, El Ghachi M, Mengin-Lecreulx D, Chippaux M, Denizot F (2005) BcrC from *Bacillus subtilis* acts as an undecaprenyl pyrophosphate phosphatase in bacitracin resistance. J Biol Chem 280:28852–28857

Eichler J, Adams MW (2005) Posttranslational protein modification in Archaea. Microbiol Mol Biol Rev 69:393–425

El Ghachi M, Derbise A, Bouhss A, Mengin-Lecreulx D (2005) Identification of multiple genes encoding membrane proteins with undecaprenyl pyrophosphate phosphatase (UppP) activity in *Escherichia coli*. J Biol Chem 280:18689–18695

Ghosh A, Shieh JJ, Pan CJ, Sun MS, Chou JY (2002) The catalytic center of glucose-6-phosphatase. J Biol Chem 277:32837–32842

Hemrika W, Renirie R, Dekker HL, Barnett P, Wever R (1997) From phosphatases to vanadium peroxidases: a similar architecture of the active site. Proc Natl Acad Sci USA 94:2145–2149

Icho T (1988) Membrane-bound phosphatase in *Escherichia coli*: sequence of the pgpB gene and dual subcelullar localization of the pgpB product. J Bacteriol 170:5117–5124

Ishikawa K, Mihara Y, Gondoh K, Suzuki E, Asano Y (2000) X-ray structures of a novel acid phosphatase from *Escherichia blattae* and its complex with the transition-state analog molybdate. EMBO J 19:2412–2423

Isupov MN, Dalby AR, Brindley AA, Izumi Y, Tanabe T, Murshudov GN, Littlechild JA (2000) Crystal structure of dodecameric vanadium-dependent bromoperoxidase from the red algae *Corallina officinalis*. J Mol Biol 299:1035–1049

Littlechild J, Garcia-Rodriguez E, Dalby A, Isupov MN (2002) Structural and functional comparisons between vanadium haloperoxidase and acid phosphatase enzymes. J Mol Recognit 15:291–296

Makde RD, Mahajan SK, Kumar V (2007) Structure and mutational analysis of the PhoN protein of *Salmonella typhimurium* provide insight into mechanistic details. Biochemistry 46:2079–2090

Manabe F, Itoh YH, Shoun H, Wakagi T (2009) Membrane-bound acid pyrophosphatase from *Sulfolobus tokodaii*, a thermoacidophilic archaeon: heterologous expression of the gene and characterization of the product. Extremophiles 13:859–865

Messerschmidt A, Wever R (1996) X-ray structure of a vanadium-containing enzyme: chloroperoxidase from the fungus *Curvularia inaequalis*. Proc Natl Acad Sci USA 93:392–396

Meyer W, Schäfer G (1992) Characterization and purification of a membrane-bound archaebacterial pyrophosphatase from *Sulfolobus acidocaldarius*. Eur J Biochem 207:741–746

Moll RG, Schäfer G (2004) Novel functional aspects of the membrane-bound exo-pyrophosphatase of the hyperthermoacidophilic archaeon *Sulfolobus* are provided by analysis of its gene and the adjacent gene cluster. J Bioenerg Biomembr 36:143–150

Neuwald AF (1997) An unexpected structural relationship between integral membrane phosphatases and soluble haloperoxidases. Protein Sci 6:1764–1767

Renirie R, Hemrika W, Wever R (2000a) Peroxidase and phosphatase activity of active-site mutants of vanadium chloroperoxidase from the fungus i. Implications for the catalytic mechanisms. J Biol Chem 275:11650–11657

Renirie R, Hemrika W, Piersma SR, Wever R (2000b) Cofactor and substrate binding to vanadium chloroperoxidase determined by UV-VIS spectroscopy and evidence for high affinity for pervanadate. Biochemistry 39:1133–1141

Stukey J, Carman GM (1997) Identification of a novel phosphatase sequence motif. Protein Sci 6:469–472

Tatar LD, Marolda CL, Polischuk AN, van Leeuwen D, Valvano MA (2007) An *Escherichia coli* undecaprenyl-pyrophosphate phosphatase implicated in undecaprenyl phosphate recycling. Microbiology 153:2518–2529

Touze T, Blanot D, Mengin-Lecreulx D (2008) Substrate specificity and membrane topology of *Escherichia coli* PgpB, an undecaprenyl pyrophosphate phosphatase. J Biol Chem 283:16573–16583

Wakagi T, Oshima T (1985) Membrane-bound ATPase of a thermoacidophilic archaebacterium, *Sulfolobus acidocaldarius*. Biochim Biophys Acta 817:33–41

Wakagi T, Oshima T (1986) Membrane-bound ATPase and electron transport system of *Sulfolobus acidocaldarius*. Syst Appl Microbiol 7:342–345

Wu S, Zhong J, Huan L (2006) Genetics of subpeptin JM4-A and subpeptin JM4-B production by *Bacillus subtilis* JM4. Biochem Biophys Res Commun 344:1147–1154